IL NUOVO CIMENTO **42 C** (2019) 38
DOI 10.1393/ncc/i2019-19038-5

COLLOQUIA: SoHe3 2018

The consequences of ICME impact on the circumterrestrial environment: A case event

M. PIERSANTI

INFN, Sezione di Roma "Tor Vergata" - Rome, Italy

received 28 December 2018

Summary. — The Solar Wind-Magnetosphere-Ionosphere coupling constitutes an important subject of scientific interest, in particular in the Space Weather context. Briefly, in this process, the energy is transferred from the solar wind to the magnetosphere by means of both the magnetic reconnection at the dayside magnetopause and the viscous-like interaction generated by micro or macro instabilities. On the other hand, the magnetosphere and the ionosphere, strictly connected through the magnetic field lines, can exchange energy and momentum, basically, through three main processes: (1) the transmission of electric fields, (2) the flows of electric charges by means of Field Aligned Current (FAC) and (3) the precipitation and/or outflow of particles. In this work, we study some aspects of the interaction of the interplanetary coronal mass ejections (ICME) of June 21, 2015 event with the magnetosphere-ionosphere system. In particular, we analyse the response of the magnetosphere to the impact of the interplanetary shock preceding the ICME, the magnetospheric and the ionospheric disturbance currents, and the geomagnetically induced currents (GIC) that developed over the entire northern hemisphere.

1. – Introduction

When an Interplanetary Coronal Mass Ejection, (ICME) hits the Earth's magnetosphere, a geomagnetic storm (GS) can be generated [1]. Usually, GSs are caused by the interaction between the magnetosphere and the ICME magnetic field. The energy coupling between them is due to the so called "magnetic reconnection" between the possible occurrence of southward interplanetary magnetic field (IMF) and the northward Earth's magnetic field [2]. In fact, [3, 4] showed that a strong and a long lasting southward IMF component ($B_{z,IMF}$) of the ICME make it highly geoeffective. In this scenario, the magnetospheric field falls into a strong disturbed state, caused by the intensification of all its current systems [5, 2, 6]: ring current, the Chapman-Ferraro current, the tail current and the auroral electrojets. The effects of this current system enhancement can be seen both at ground and in the near Earth-space [7-9, 4]. The strength of GSs is typically measured

by the Dst index [3], which is considered to reflect the variations in the intensity of the symmetric part of the ring current [10].

[11, 12, 4, 13] showed that, during a GS, the convection electric field generated in the magnetosphere causes a global ionospheric current responsible for the disturbance of polar field 2 (DP2) magnetic variations at both high latitude and dayside geomagnetic equator. A similar DP2-type ionospheric currents has been identified during geomagnetic sudden impulse (SIs) [14,12,4] and global Pc 5 pulsations [15]. The SI generally precedes the main phase of a geomagnetic storm and indicates the arrival of the interplanetary fast shocks or discontinuities of the incoming solar wind (SW) colliding with the magnetopause and compressing the magnetosphere [14, 12]. The behaviour of SIs at geosynchronous orbit and in the outer magnetosphere have been studied in several works [16, 17, 7, 12, 13]. Here, the SI amplitude depends on local time (LT), with highest values around noon and very small values (or even negative, in some cases) in the night sector. At ground the SI presents a more complex behavior, depending upon LT and geomagnetic latitude. The total disturbance field (D_{SI}) associatesd to a SI can be decomposed into different subfields, namely $D_{SI} = DL + DP$ [14]. They consist of a step-like structure of magnetospheric origin dominant at low latitudes (DL field, where L stands for low latitude) and a double pulse structure of ionospheric origin (DP field, where P stands for polar latitude), dominant at high latitudes; the first and the second pulse are called preliminary impulse (PI) and main impulse (MI), respectively. The DP fields generates in ionosphere a double cell vortices (one in the morning sector and one in the afternoon sector) for both the PI and MI [14, 12, 18].

Generally, at ground a GS can be divided into three phases [3]: initial, main and recovery. The initial phase is characterized the a sudden increase in the geomagnetic field by 20 to 50 nT in tens of minutes (SI). The main phase is defined by decreasing of the geomagnetic field to its minimum value, caused by the intensification of the ring current. The duration of the main phase varies typically between 2 to 8 hours. The recovery phase is when the geomagnetic field changes from its minimum value to its quiet time values. The recovery phase may last as short as 8 hours or as long as 7 days.

2. – The June 22, 2015 case event

Figure 1 shows the ICME observations by WIND spacecraft (1^{st} Lagrangian point). Four interplanetary shocks (IP) was observed at 16:05 UT on 21 June (IP1), 05:02 UT (IP2) and 18:07 UT(IP3) on 22 June and 13:12 UT (IP4) on 24 June, respectively. The first shock was caused by the 18 June CME while the second shock was driven by a CME from 19 June [4]. In addition, the ICME (and its preceding shock - IP3) were produced by the 21 June CME and the fourth shock (IP4) was associated with the 22 June CME [4]. The ICME boundaries are determined by the decrease in the temperature coupled with a smooth rotation of the magnetic field.

At ground, on 22 June at 18:37 UT, SYM-H shows a large SI, directly related to the increase of the SW speed and proton density (fig. 1, panel h). After the first rapid decrease of SYM-H (at 20:17 UT), a large negative peak (SYM-H = −208 nT) was observed on 23 June at 04:27 UT. This structure resembles the $B_{z,IMF}$ component behaviour, caracterized by two periods of nearly stable negative values. As a consequence, the SW plasma can flow inside the Earth's magnetosphere because of the occurrence of the magnetic reconnection process between the IMF and Earth's magnetic field. At high latitude, the geomagnetic activity is characterized by large bursts of activity (AE-index, panel i). This is the evidence of the activity in the geomagnetic tail, due to the so-called

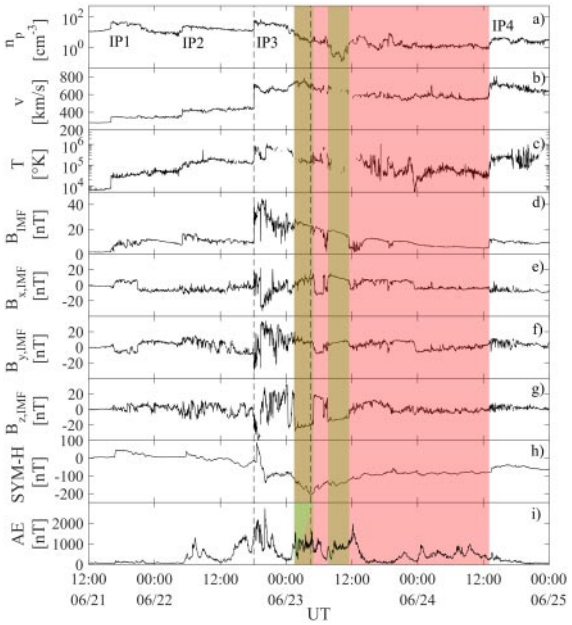

Fig. 1. – Solar wind parameters as measured at L1 position by WIND spacecraft: a) proton density; b) velocity; c) proton temperature; d) IMF intensity; e-g) IMF x, y, z components in GSE coordinate system. Panel h and Panel i show SYM-H and AE indices, respectively, between 21 June and 24 June 2015. The two dashed lines indicates the ICME associated shock as observed by WIND on 22 June at 17:59 UT (IP3) and the minimum values reached by SYM-H during the storm main phase on 23 June at 04:27 UT. The white area behind the IP3 shock is the sheath, while the red shaded region corresponds to the overall ejecta interval. The green shaded regions show two small magnetic clouds and/or fluxropes identified within the ICME [4].

loading-unloading process [6]. Moreover, the high latitude geomagnetic activity continues also during the first part of the GS recovery phase, probabyl due to the successive negative turnings of the $B_{z,IMF}$ (green shaded regions in fig. 1), occurring on 23 June after the 10:00 UT.

Figure 2 shows the SW and the IMF WIND observations (box a), and the magnetospheric field observations (box b) by GOES13 (LT=UT-5) and GOES15 geosynchronous spacecrafts (LT=UT-9). The IP3 shock was characterized by a huge variation of both the SW pressure (ΔP_{SW} ∼31.5 nPa) and IMF strength (ΔB_{IMF} ∼22.3 nT), associated with a great negative $B_{z,IMF}$ (∼-20.0 nT), persisting for ∼90 min. The SI was observed by both GOES at ∼18:33 UT (box b) and was characterized by small and rapid enhancement in the B_z ($B13_z$ and $B15_z$ in GSM coordinate system) component before a sharp transition from ∼100 nT to ∼-100 nT; at the same time the other components undergo strong variations. These features are indicative of magnetopause crossing [19]. In fact, the predicted configuration of the magnetospheric field lines in the noon/midnight plane, before (black lines) and after (red lines) the shock impact (TS04 model, [20]), reveals the extreme field compression.

In order to evaluate the ionospheric current pattern associated to the SI of 22 June 2015, the [12] model was applied to 63 ground magnetic observatories in the northern hemisphere. The global results for PI_{IC} and MI_{IC} vectors, are showed in fig. 3. Panel

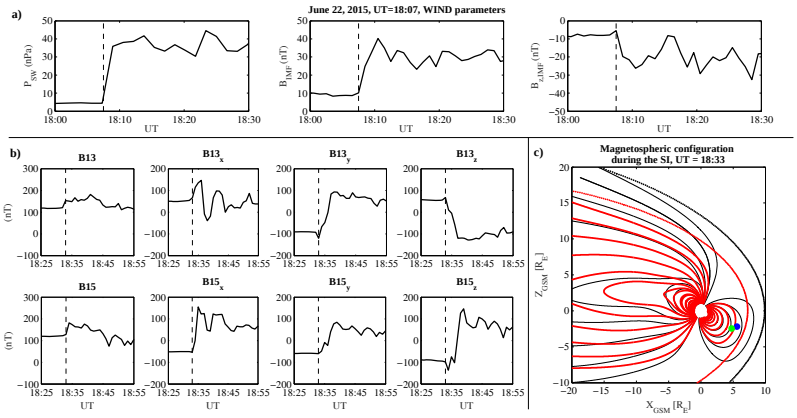

Fig. 2. – SW parameters as measured by WIND: box a) dynamic pressure, total magnetic field, Z_{SM} component of the IMF. Box b) The magnetic field magnitude and components in the GSM coordinate system as measured by GOES13 and GOES15. Box c) The position of the two geosynchronous satellites and the magnetospheric configuration before (black lines) and after (red lines) the shock impact [4].

a) and panel b) show the direction of the ionospheric current for the PI_{IC} and the MI_{IC}, respectively. Their behavior are consistent with a morning counter-clockwise (CCW) and an afternoon clockwise vortices (CW) for the PI_{IC} and a morning CW and an afternoon CCW vortices for the MI_{IC}, respectively. These results are in agreement with [14] and

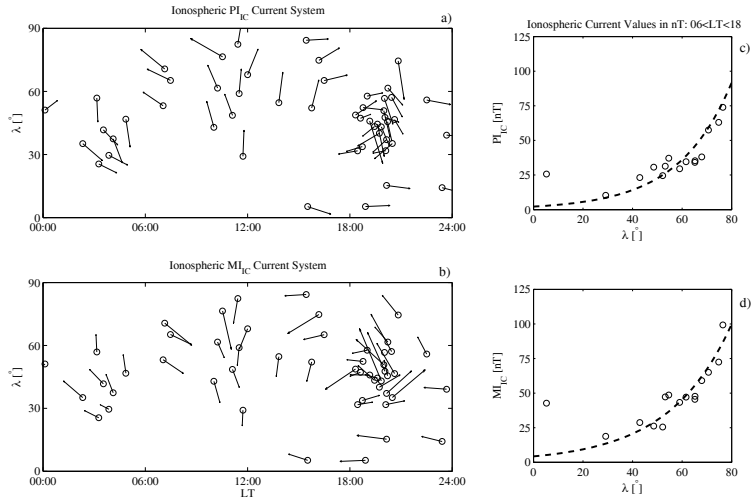

Fig. 3. – Panels a) and b): the direction of the ionospheric currents for the PI_{IC} (a) and for the MI_{IC} (b), as a function of latitude and local time after a 90° rotation of the disturbance magnetic field. Panels c) and d): the characteristics of the PI_{IC} (c) and MI_{IC} (d) amplitude fields as a function of latitude in the dayside sector (06<LT<18); dashed lines represent the exponential fits and black circles represent the morning PI_{IC} and MI_{IC} [4].

with [12]. Panels c and d show the amplitude of the PI_{IC} and MI_{IC} fields *vs* latitude in the dayside sector (06<LT<18). In agreement with [12], both PI_{IC} and MI_{IC} field amplitudes increase with latitude and the experimental points can be approximated by an exponential function (black dashed lines).

3. – Conclusions

The understanding of the magnetospheric and ionospheric plasma dinamics continues to be one of the key point in the Space Weather contexct. The structures of the magnetospheric current system and how it couples with the ionospheric medium continues to be the subject of intense discussions [21, 22]. This core area of magnetospheric-ionospheric physics is very important in the understanding the nature of magnetospheric storms and substorms. The June 2015 GS represents a nice example of the SW-magnetosphere-ionosphere coupling in terms of current systems developing. The analysis presented here shows that a remarkable interplanetary shock was observed at L1 point at 18:07 UT, on 22 June 2015. The magnetospheric response to the shock arrival (18:33 UT) was characterized by a great erosion of the magnetopause because of the strong southward component of B_{IMF}. On 22 June at 18:37 UT large SI (up to 88 nT) was observed at ground preceding the geomagnetic storm occurred on 22 June. Both the PI_{IC} and the MI_{IC} produced a twin ionospheric current vortices that completely modified the quiet ionospheric current pattern. These results are in agreement with [14] and with [12].

* * *

The author thanks the national institutes that support them and INTERMAGNET for promoting high standards of magnetic observatory practice (www.intermagnet.org). The author kindly acknowledges N. Papitashvili and J. King at the National Space Science Data Center of the Goddard Space Flight Center for the use permission of 1-min OMNI data and the NASA CDAWeb team for making these data available. The author also thankd the Italian Space Agency (ASI) for the financial support under the contract ASI "LIMADOU scienza" n° 2016-16-H0.

REFERENCES

[1] Tsurutani B. T. and Lakhina G. S., *Geophys. Res. Lett.*, **41** (2014) 2.
[2] Dungey J. W., *Phys. Rev. Lett.*, **6** (1961) 2.
[3] Gonzalez W. D., Joselyn J. A., Kamide Y., Kroehl H. W., Rostoker G., Tsurutani, B. T. and Vasyliunas, V. M., *J. Geophys. Res-Space*, **99** (1994) A4.
[4] Piersanti M. et al., *Sol. Phys.*, **292** (2017) 11.
[5] Daglis I. A., Axford W. I., Sarris E. T., Livi S. and Wilken B., *Sol. Phys.*, **172** (1997) 1.
[6] Consolini G. and De Michelis P., *Geophys. Res. Lett.*, **32** (2005) 5.
[7] Villante U. and Piersanti M., *J. Geophys. Res-Space*, **114** (2010) A6.
[8] Vellante M., Piersanti M. and Pietropaolo E., *J. Geophys. Res-Space*, **110** (2005) A3.
[9] Vellante M., Piersanti M., Heilig B., Reda J. and Del Corpo, A., *2014 XXXIth URSI General Assembly and Scientific Symposium (URSI GASS)*, **1** (2014) 4.
[10] Dessler A. J. and Parker E. N., *J. Geophys. Res-Space*, **64** (1959) 12.
[11] Alberti T., Piersanti M., Vecchio A., De Michelis P., Lepreti F., Carbone V. and Primavera L., *Ann. Geophys.*, **34** (2016) 11.
[12] Piersanti M. and Villante U., *J. Geophys. Res-Space*, **121** (2016) 7.

[13] Piersanti M., Cesaroni C., Spogli L. and Alberti T., *Adv. Space Res.*, **60** (2017) 8.
[14] Araki T., *Geoph. Monog. Series*, **1** (1994) 5.
[15] Piersanti M., Villante U., Waters C. and Coco I., *J. Geophys. Res-Space*, **117** (2012) A2.
[16] Kokubun S., *J. Geophys. Res-Space*, **88** (1983) A12.
[17] Lee D. Y. and Lyons L. R., *J. Geophys. Res-Space*, **109** (2004) A4.
[18] Carter B. A., Yizengaw E., Pradipta R., Weygand J. M., Piersanti M., Pulkkinen A., Moldwin M. B., Norman R. and Zhang K., *J. Geophys. Res-Space*, **121** (2016) 10.
[19] Suvorova A., Dmitriev A., Chao J. K., Thomsen M. and Yang, Y. H., *J. Geophys. Res-Space*, **110** (2005) A1.
[20] Tsyganenko N. A. and Sitnov M. I., *J. Geophys. Res-Space*, **119** (2014) 4.
[21] Ganushkina N.Y. et al., *Ann. Geophys.*, **33** (2015) 1369.
[22] Piersanti M., Materassi M., Cicone C., Spogli L., Zhou H. and Ezquer R. G., *J. Geophys. Res-Space*, **123** (2018) 1.